

## Article

# Effect of Different Combustion Modes on the Performance of Hydrogen Internal Combustion Engines under Low Load

Wei Wei <sup>1,2</sup>, Xu He <sup>1</sup>, Hairong Zhu <sup>3,\*</sup>, Junfa Duan <sup>2,\*</sup> and Gaolin Qin <sup>2</sup>

<sup>1</sup> School of Mechanical Engineering, Beijing Institute of Technology, Beijing 100081, China; weiwei86@ncwu.edu.cn (W.W.); hhexxu@bit.edu.cn (X.H.)

<sup>2</sup> School of Mechanical Engineering, North China University of Water Resources and Electric Power, Zhengzhou 450045, China; qingaolin@ncwu.edu.cn

<sup>3</sup> School of Mechanical Engineering, Hebei University of Science and Technology, Shijiazhuang 050018, China

\* Correspondence: zhuhr@hebest.edu.cn (H.Z.); djf@ncwu.edu.cn (J.D.); Tel.: +86-1803-1670-865 (H.Z.)

**Abstract:** Detailed hydrogen–air chemical reaction mechanisms were coupled with the three-dimensional grids of an experimental hydrogen internal combustion engine (HICE) to establish a computational fluid dynamics (CFD) combustion model based on the CONVERGE software. The effects of different combustion modes on the combustion and emission characteristics of HICE under low load were studied. The simulation results showed that, with the increase in excess hydrogen, the equivalent combustion and excessive hydrogen combustion modes with medium-cooled exhaust gas recirculation (EGR) dilution could improve the intensity of the in-cylinder combustion of HICE, increase the peak values of pressure and temperature in the cylinder, and then improve the indicated thermal efficiency of HICE under low load. However, larger excessive hydrogen combustion could weaken the improvement in performance; therefore, the performance of HICE could be comprehensively improved by the adoption of excessive hydrogen combustion with a fuel–air ratio below 1.2 under low load. The obtained conclusions indicate the research disadvantages in the power and emission performances of HICE under low load, and they are of great significance for the performance optimization of HICE. Furthermore, a control strategy was proposed to improve the stability of HICE under low load.

**Keywords:** hydrogen internal combustion engine; lean combustion; equivalent combustion; excessive hydrogen combustion; combustion characteristic; NO<sub>x</sub> emissions



**Citation:** Wei, W.; He, X.; Zhu, H.; Duan, J.; Qin, G. Effect of Different Combustion Modes on the Performance of Hydrogen Internal Combustion Engines under Low Load. *Sustainability* **2022**, *14*, 6095. <https://doi.org/10.3390/su14106095>

Academic Editor: Talal Yusaf

Received: 14 March 2022

Accepted: 3 May 2022

Published: 17 May 2022

**Publisher's Note:** MDPI stays neutral with regard to jurisdictional claims in published maps and institutional affiliations.



**Copyright:** © 2022 by the authors. Licensee MDPI, Basel, Switzerland. This article is an open access article distributed under the terms and conditions of the Creative Commons Attribution (CC BY) license (<https://creativecommons.org/licenses/by/4.0/>).

## 1. Introduction

### 1.1. Research Background

Energy resources are among the bases on which human beings depend for survival. In 2020, primary energy and carbon emissions fell at the fastest rate since World War II due to the COVID-19 pandemic, while overall oil demand declined, according to BP's 2021 Statistical Yearbook of World Energy [1]. With the continuous strengthening of people's understanding of energy and environmental pollution, the world energy structure is gradually changing from a single energy-type to diversified energy-types.

Automobile exhaust emissions produce large amounts of carbon monoxide (CO), carbon dioxide (CO<sub>2</sub>), hydrocarbons (HC), nitrogen oxides (NO<sub>x</sub>), and other contaminants [2], which harm the human respiratory system, cardiovascular system, nervous system, immune function, and reproductive function. Urban air pollution has become an important public health risk [3–7]. The ecological environment in China is seriously harmed by pollution from traditional fuels, which also restricts the development of higher-quality products in China's economy.

It is very difficult for the automobile industry to improve the combustion control of internal combustion engines and the fuel economy of traditional internal combustion engines so as to reduce fuel consumption and the emission of pollutants. In order to deal with energy and environmental problems, searching for automotive clean alternative fuels

and breaking the traditional pattern of fuel combustion engines has gradually become the main direction for dealing with energy crises and environmental problems [8,9].

At present, there are mainly alcohol-based alternative fuels, ether alternative fuels, natural gas, liquefied petroleum gas (LPG), biomass diesel, hydrogen, and other alternative fuels for vehicles [10].

When alcohol fuel is used as engine fuel, the dynamic performance of automobiles is reduced due to the higher latent heat of vaporization and lower fuel calorific value [11]. In general, when blended fuel is used as engine fuel, the power performance of the internal combustion engine usually does not change much [12–14]. Ethanol, as an alternative fuel for automobiles, has a high production cost and can be widely promoted only after the production technology is greatly improved. Methanol automobiles have poor start performance and unstable ignition under low-temperature conditions. Under low load conditions, they discharge a large amount of formaldehyde and methanol and cause corrosion to metals and nonmetals [15–18].

Ether substitute fuel mainly refers to dimethyl ether. Its performance is stable, it is not prone to oxidation, it is noncorrosive, high in oxygen content with excellent combustion characteristics, and it does not produce soot under different working conditions [19]. However, the direct use of dimethyl ether as an internal combustion engine fuel causes wearing of parts and affects reliability [20–22].

The main component of natural gas is methane, which is rich in resources, and natural gas contains a large amount of it. The content of harmful substances, such as CO and HC, in the products after combustion is relatively small, resulting in a minor impact on the environment [23,24]. Compared with gasoline and diesel, the combustion efficiency is high, the safety performance is good, and the pollutants and CO<sub>2</sub> generated after combustion are greatly reduced [25,26]. At present, it has become an internationally recognized important means for automobile energy conservation and emission reduction. However, the natural gas engine is not easy to ignite under the condition of a cold start, spontaneous combustion of the mixture occurs under low load, and detonation occurs easily under high load [27]. Therefore, the combustion of a natural gas engine can only run stably within the range of a medium load.

Biomass diesel is a kind of new and renewable energy. It is biodegradable and nontoxic, its combustion performance is excellent, and it has low sulfur, hydrocarbon, and NO<sub>x</sub> emissions [28]. Biomass diesel fuel and diesel have similar physical and chemical properties, and their combustion characteristics are also relatively similar; the power performance of biomass diesel is thus not different from that of a traditional internal combustion engine, and it can be used as a substitute for diesel. Moreover, biomass diesel has the ability to soften and degrade rubber, and the engine and oil circuit seals cause certain damage [29]. Hydrogen as a kind of secondary energy has a high calorific value as well as a low ignition energy and a rapid flame propagation speed; when using it as a vehicle substitute fuel, high power and efficiency can be obtained [30]. Hydrogen molecules have only H–H bonds, and when they are fully burned, only water can theoretically be produced. This can be decomposed into hydrogen and oxygen, making hydrogen the cleanest energy source [31,32]. Hydrogen can be produced from a wide range of sources, not least through the electrolysis of water using electricity generated from various renewable energy sources such as solar, wind, and tidal power [33]. It can also be produced from organic crops, waste straw, and microbial decomposition in the organic wastewater treatment process. It is considered by researchers to be the ideal fuel for an internal combustion engine.

There are two main methods for the application of hydrogen energy in cars: one is to make hydrogen fuel cells and generate electrical energy through electrochemical reactions; the other is to directly use it as a fuel in an internal combustion engine cylinder. When generating electrical energy directly with electrochemical reactions, hydrogen fuel cells transform the chemical energy of the hydrogen fuel directly into electricity, resulting in high energy efficiency, stable working conditions, no environmental pollution, and a consequent reduction in environmental pollution [34]. However, its very high requirement

for hydrogen purity, as high as 99.99%, and security and storage of hydrogen fuel efficiency has become an important challenge in the development of hydrogen fuel cell [35,36]. The hydrogen fuel cell is limited by cost and technology. The development of hydrogen fuel cell involves the core components of proton exchange membrane, precious metals, platinum catalyst, material is expensive, and the resources are scarce [37]. At present, China does not have industrialization ability for key materials such as catalyst, bipolar plate, and key components such as a high-pressure hydrogen storage tank and a hydrogen circulation pump [38]. Due to the high cost and the performance and service life of a hydrogen fuel cell, it is difficult to meet the needs of the whole society through large-scale and industrial production in the foreseeable time. HICE works on the same principle as traditional internal combustion engine. HICE can be obtained by adding a hydrogen supply system to the traditional internal combustion engine and slightly modifying the ignition system [39]. At present, the technology of HICE is relatively mature and its cost of research and development is also relatively low [40]. The maintenance of HICE is the same as that of traditional internal combustion engine, which is easy to be accepted by the majority of users.

### *1.2. Development Status of HICE*

HICE has many advantages over petroleum fuel engines. For example, [41], (1) Hydrogen flame propagation speed and combustion in the engine antidetonating quality is better than gasoline, and can use a higher compression ratio, so the thermal efficiency is higher than while burning gasoline; (2) hydrogen has a wider ignition boundary than gasoline, which makes it easy to achieve lean combustion and improve economy. Meanwhile, it can reduce the maximum combustion temperature and greatly reduce  $\text{NO}_x$  emissions; (3) hydrogen mixture ignition energy is low, easy to ignite, almost never catches fire when working, with good start-up.

The combustion speed of hydrogen in the cylinder of HICE is fast, the temperature in the cylinder is high, and the cylinder wall and other components lose a lot of heat, which all make the efficiency of HICE lower than that of fuel cell. In practice, hydrogen fuel cells have high efficiency only under low load. With the increase in load, the output current of fuel cells increases, and the heat loss increases exponentially with the increase in current. Under high load, fuel cells are almost as efficient as internal combustion engines.

Hydrogen fuel cell is considered by many experts and scholars as the ultimate way to use hydrogen as energy in automobiles. However, the technical and cost problems of hydrogen fuel cell are difficult to solve in a short time. At present, HICE still has very important research significance.

After a long development time, there are still some problems to be solved in the research of HICE. The current research on HICE mainly focuses on the chemical reaction mechanism, combustion characteristics in the cylinder of HICE, and the  $\text{NO}_x$  generation rule, among which the research on combustion characteristics in the cylinder of HICE and  $\text{NO}_x$  generation rule is of great significance.

Ma Fanhua et al. [42] tested the in-cylinder combustion characteristics of HICE under different working conditions, and studied the effects of ignition advance angle, rotational speed, and load on the in-cylinder combustion characteristics. The results show that ignition advance angle has little effect on indicating efficiency of HICE. HICE can burn in time at low and medium speeds and adapt to different speeds; throttle opening will affect the amount of residual exhaust gas in the cylinder of HICE, and then the concentration of hydrogen in the cylinder, and the combustion speed in the cylinder of HICE, so that the indicating thermal efficiency and cycle variation of HICE will change.

Liu Fushui et al. [43,44] conducted an experimental study on the cycle variation and influencing factors of HICE. The results show that the cycle variation coefficient of average indicated pressure is an important parameter to characterize the cycle variation characteristics of HICE. The higher speed of the hydrogen engine at idle speed, the smaller the cycle change; the cycle variation of HICE decreases with the increase in mixture

concentration. In the process of HICE at idle, the speed of the air-intake spray hydrogen produces a great impact on the cyclic variations.

Ji Changwei et al. [45] conducted bench experiments on gasoline hydrogen-doped internal combustion engines with different volume fractions of hydrogen mixture, and conducted simulation studies on hydrogen internal combustion engines with AVL Boost software under different combustion conditions. The results show that mixing hydrogen can increase the combustion speed, shorten the flame development period and propagation period, increase the peak value of the pressure in the cylinder, and improve the combustion condition.

Sun Dawei et al. [46] conducted experiments based on four-cylinder HICE to study the combustion and emission characteristics of EGR-degree HICE. The results show that the fuel to air ratio can be changed by adjusting EGR when the hydrogen injection volume is kept constant. Under low load, hot EGR can increase the temperature in the cylinder and increase NO<sub>x</sub> emission. Under high load, hot EGR can significantly reduce NO<sub>x</sub> emissions at slightly higher mixture concentrations.

The usage of the hot EGR method can make the combustion of HICE longer in duration and reduce temperature and pressure in the cylinder. Increasing the EGR rate can reduce the in-cylinder temperature and combustion speed, and the NO<sub>x</sub> emission can be greatly reduced, but too large an EGR rate can greatly reduce the power performance and economy of HICE [47–49].

Fan Yingjie [50] has set up a platform of planar-laser-induced fluorescence test. Using the OH-PLIF method, hydrogen–air premixed combustion products produced in the middle of the hydroxyl were collected, tested, and analyzed. The results show that the increase in concentration and temperature can promote the formation of hydroxyl groups, while the increase in pressure has a complicated effect on the formation of hydroxyl groups, but also has a trend of promoting the formation. The use of EGR can effectively inhibit combustion and reduce nitrogen oxide emissions, and the role of hot EGR is stronger.

Hao Jiatian [51] conducted EGR technology-simulation analysis based on a one-dimensional model of HICE, and analyzed the effect of Miller cycle technology on detonation and NO<sub>x</sub> emission suppression. Finally, the combination of the two technologies can effectively improve the compression ratio and thermal efficiency of HICE while reducing NO<sub>x</sub> emissions.

Sharma [52,53] studied the characterization of the HICE under dual fuel (DF) mode. Hydroxy gas (HHO) is supplied along with diesel at three different flow rates. The results show that CO and smoke emissions are significantly reduced under DF mode, and brake thermal efficiency (BTE) and brake-specific energy consumption (BSEC) of HICE are also improved. At the same time, the high temperature in the cylinder can increase the oxidation rate of fuel types, thus reducing HC, CO, and smoke emissions, but also increasing NO<sub>x</sub> emissions.

In the conditions of idle and low load, the indicated power of an internal combustion engine is mainly used to overcome the heat loss and external resistance, so only a small amount of fuel is needed. The decrease in fuel and the constant supply of air will cause the mixture concentration in the cylinder of the internal combustion engine to be too low, near or below the lean combustion limit of the mixture, and the mixture is not easy to ignite; while the flame propagation rate is very low, the cyclic variation in the cylinder will increase, and the engine work will be unstable. Reducing the supply of air can increase the concentration of the hydrogen–air mixture; away from the lean combustion limit, the usage of EGR technology can obtain equivalent combustion or excessive hydrogen combustion to reduce the possibility of a HICE fire under idle and low loads and improve the working stability. However, the usage of EGR technology would reduce the charge coefficient and increase the residual exhaust gas in the cylinder, which may also greatly reduce the flame propagation velocity and affect the indicated efficiency. Therefore, more research is needed on which combustion mode can make HICE obtain a higher indicated power and indicated efficiency under low load.

In this paper, based on the experimental port fuel injection (PFI) HICE of Beijing Institute of Technology, a CFD simulation model of three-dimensional entity grid coupling detailed H-O-N reaction mechanism was established, calibrated, and verified by previous experimental data. The effects of lean combustion, equivalent combustion (with medium-cooled EGR dilution), and excessive hydrogen combustion (with medium-cooled EGR dilution) on in-cylinder combustion and emission characteristics of HICE under low load were studied. The obtained conclusions make up research disadvantages of power and emission performances of HICE under low load, and are of great significance for the performance optimization of HICE. Furthermore, a control strategy was proposed to improve the stability of HICE under low load.

## 2. Materials and Methods

### 2.1. Three-Dimensional Model of HICE

A three-dimensional (3D) simulation model of the PFI HICE with four cylinders and four strokes was established [49,54], and its main parameters are shown in Table 1.

**Table 1.** Main parameters of HICE.

Parameters	Value
Fuel type	Hydrogen
Ignition mode	Spark ignition
Displacement/L	2.0
Fuel supply mode	Port fuel injection
Cylinder number	4
Bore/mm	86
Stroke/mm	86
Compression ratio	10:1
Intake valve open degree	−368 °CA
Intake valve close degree	−128 °CA
Exhaust valve open degree	−560 °CA
Exhaust valve close degree	−354 °CA

The experimental HICE had four cylinders, the difference among which was ignored to simplify the model. The three dimensions (3D) entity model we built consisted of one surge tank, one inlet, one cylinder, two intake valves, two exhaust valves, and a hydrogen injection valve, as shown in Figure 1. The 3D model file in STL format was imported into the CONVERGE Studio. After detecting and repairing the geometric surface of the model and then defining the boundary type and boundary condition of each region, the surface grid file of surface.dat was generated. In the simulation process, the software automatically generated the grid based on the preset grid-generation rules.

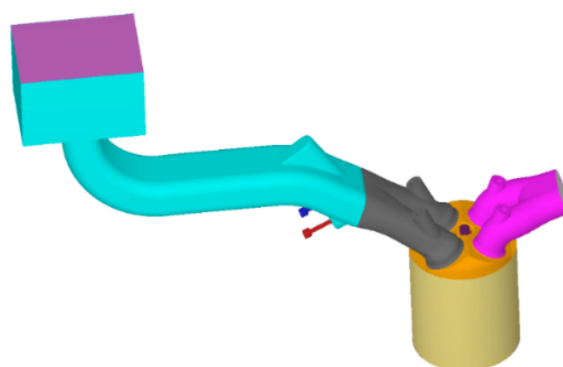


**Figure 1.** Entity model of HICE.

The Converge software automatically generated Cartesian computational grids in the process of calculation via preset basic grid length and refine rules. In this paper, the basic

grid length is 8 mm, the encryption levels in intake, exhaust pipe and cylinder are two, and their grid sizes are 2 mm. The encryption levels near spark plug and flame front surface are five, and their grid sizes are 0.25 mm. The adaptive encryption levels of temperature and speed are four, and their grid sizes are 0.5 mm. There are more than 420,000 maximum grid numbers of the CFD model under the combustion and injection period.

## 2.2. CFD Model and Reaction Mechanism

The combustion model adopted in this paper is the SAGE model of 3D grid coupling with a chemical reaction mechanism, which can automatically generate the encrypted dynamic grids during simulation and has a high accuracy of numerical calculation. The RNG  $k-\epsilon$  high Reynolds number flow model and the fluid–solid coupled conjugate heat transfer model used here also have high stability and convergence [49,55].

The H-O reaction mechanism adopted in this paper is the detailed sub-mechanism of GRI\_3.0 mechanism [55], which has been proven to have better prediction accuracy. The  $\text{NO}_x$  reaction mechanism in this paper includes reaction routes consisting of NO,  $\text{N}_2\text{O}$ , and  $\text{NO}_2$ , among which the NO mechanism includes three routes of thermal NO, NNH-NO,  $\text{N}_2\text{O}$ -NO, and its prediction accuracy is obviously higher than that of traditional thermal NO.

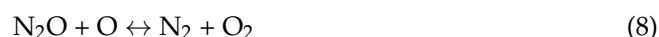
The thermal NO path contains three elementary reactions:



The NNH-NO path contains three elementary reactions:



The  $\text{N}_2\text{O}$ -NO path contains four elementary reactions:



The combustion continues only when the local temperature is greater than the self-ignition temperature of hydrogen, and the ignition energy is added to the grids of the spark plug area in simulation. The start trigger of the reaction mechanism was set as 858 K in the combustion model; when the temperature of any grid rose above 858 K, the hydrogen–oxygen reaction started. The initial temperatures of the piston and cylinder wall were set to 500 K, the temperature of the spark plug was 550 K, and the temperature of the spark plug electrode was 600 K. The simulation step size was set as 0.01 °CA and the limit of convergence was set as  $10^{-4}$ – $10^{-8}$ . In simulation, the engine speed remained constant at 3000 r/min and the throttle remained fully open. The fuel–air ratio varied from 0.2 to 1.8, and the ignition time was set between 15 °CA and  $-2$  °CA BTDC.

## 2.3. Model Verification

The simulation model was verified by the previous experimental data in reference [49,54]. The experimental data were compared with simulation results, as shown in Figure 2, which shows the in-cylinder pressure curves of simulation and experimental data at the speed

of 3000 r/min and the equivalent fuel–air ratio of 0.6, 0.8, and 1.0. It can be seen that the in-cylinder pressure curves from simulation match well with that from the experiment, among which the peak value of the in-cylinder explosion pressure from simulation calculation is slightly higher than experimental data, and the error of average pressure is less than 5%.

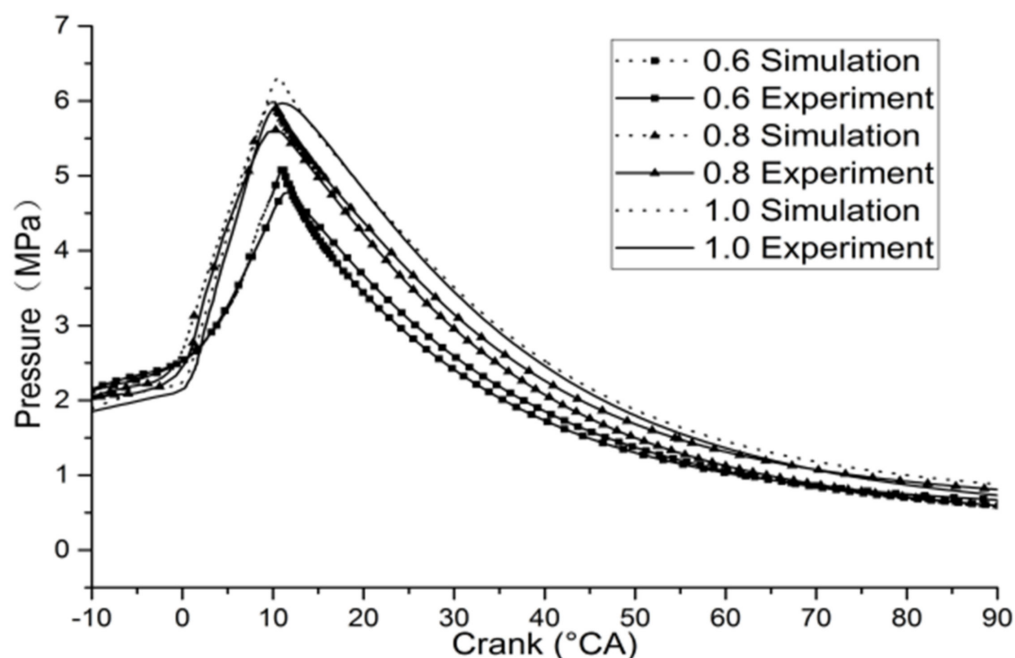


Figure 2. Verification curve of in-cylinder pressure.

### 3. Results

#### 3.1. Combustion Characteristics

##### 3.1.1. Variation of OH Concentration

OH is the most important procedural element of the H-O reactions and is always used to reveal the combustion process and to describe the combustion intensity. Figure 3 shows the slice of the spatial distribution of OH concentration in the cylinder when the fuel combustion was 5%, 50%, and 95% at the loading rate of 20% and 25%, respectively. The flame spreads to the lower part of the cylinder with the piston, and the slice of OH distribution located 5 mm above the piston top and parallel to the piston top.

According to Figure 3, OH was mainly distributed on the front surface of the flame, and the concentration of OH was the highest on the front surface. Due to the influence of the internal structure of the cylinder, such as the spark plug, an irregular flame shape appears in the center of the cylinder when the fuel burns at 5%. As the combustion continues, the flame spreads rapidly from the center of the cylinder to all sides, and the flame radius expands rapidly. The outside of the flame is the unburned zone; the OH concentration is zero, the inside of which is the burned zone. The closer to the center of the burned zone, the more complete the fuel combustion is, and the OH concentration spreads from the center of the burned zone to the front of the flame.

When the fuel burns at 5% in lean combustion, the reason why there is no flame change in the slice diagram is that the combustion process is slow and the OH concentration on the front of the flame is very low. When the fuel burns at 50%, some high-concentration OH regions appear on the front of the flame, and when the fuel combustion is 90%, the high-concentration OH regions become continuous. This shows that at low load, the flame burns slowly and discontinuously in the early stage of lean combustion, and the burning intensity increases in the later stage of combustion.

Under low load, when the loading rate is 20% and the fuel combustion is 5% and 50%, the OH concentration is the highest and the flame front is the thickest in equivalent

combustion and excessive hydrogen combustion. The OH concentration on the front surface of the excessive hydrogen combustion flame gradually decreases, and the thickness of the front surface of the flame gradually becomes thinner; as the fuel combustion is 95%, OH concentration is highest at the front of the rarefied flame. With the increase in excess hydrogen, the OH concentration on the front of the equivalent combustion and the intensified combustion flame decreases continuously.

When the loading rate is 25%, the OH concentration on the front surface of the flame is higher and thicker than that of lean combustion, and the OH concentration on the front surface of the flame of the excessive hydrogen combustion is lower than that of equivalent combustion. When fuel combustion is greater than 50%, the OH concentration on the front surface of rarefied combustion flame is the highest, the equivalent combustion and excessive hydrogen combustion gradually decrease, and the thickness of the front surface of flame becomes thinner. It shows that the equivalent combustion and excessive hydrogen combustion are more intense than lean combustion under low load, and the lean combustion is more concentrated when the fuel combustion is 95%.

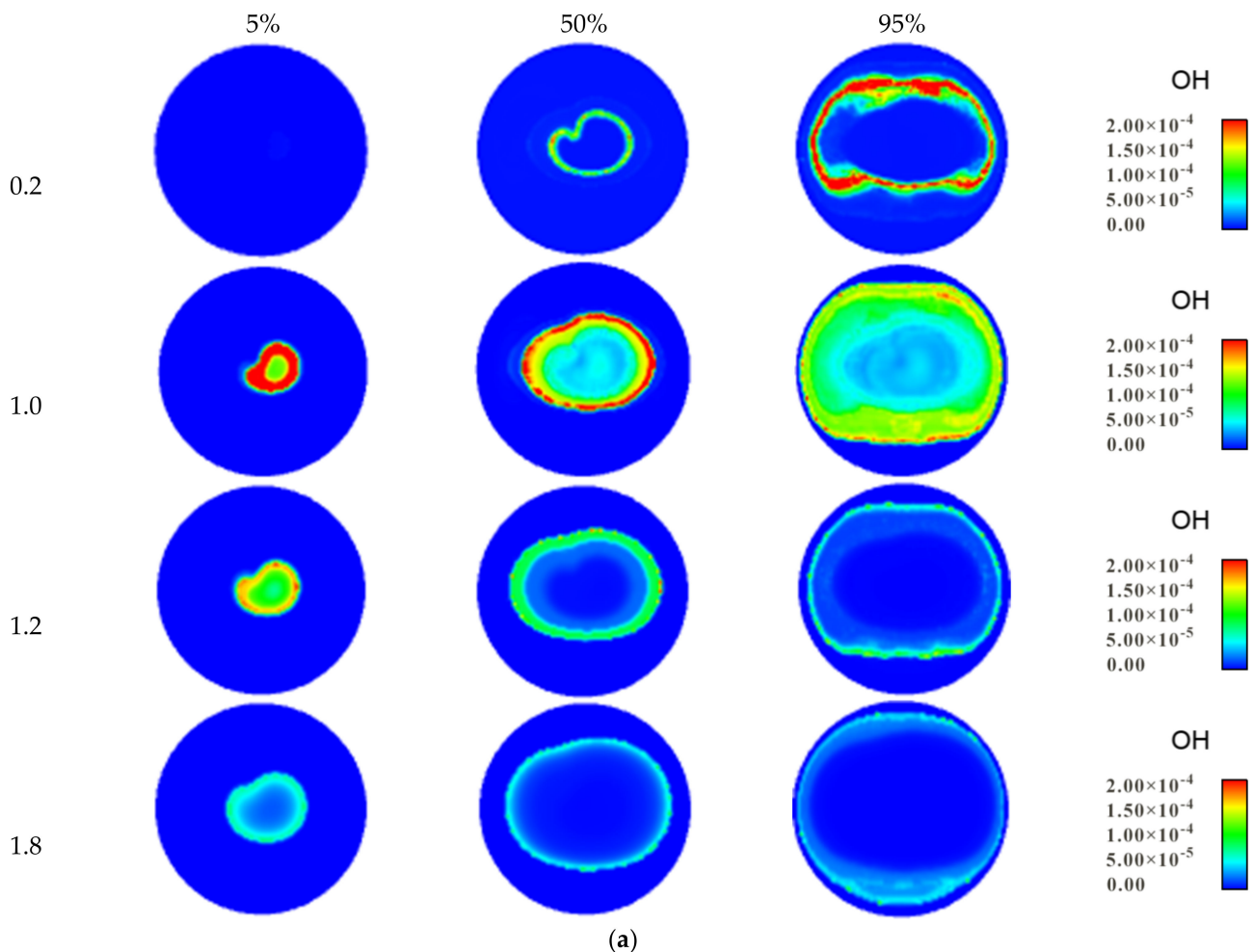
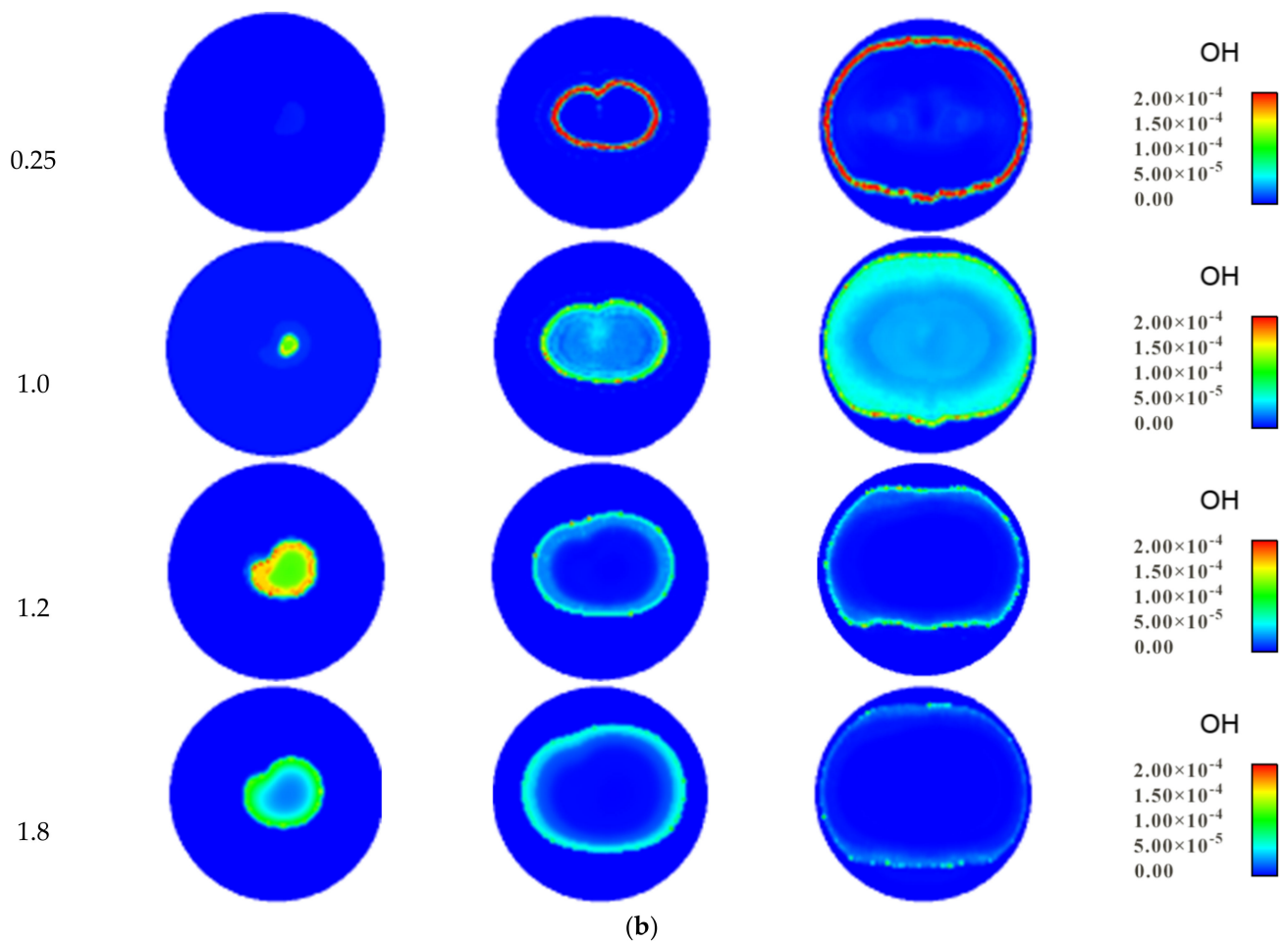


Figure 3. Cont.



**Figure 3.** OH concentration distribution in cylinder in different combustion modes under low load. (a) Loading rate of 20%; (b) loading rate of 25%.

Figure 4 shows the variation of in-cylinder OH concentration changing with the crankshaft angle in different model of combustion under low load. It can be seen that when the fuel–air ratio is 0.2, the maximum OH concentration is 116 ppm at the crankshaft angle of  $-0.8^{\circ}\text{CA}$ . Equivalent combustion with EGR rate of 75.2% at a crankshaft angle of  $-4.91^{\circ}\text{CA}$  produces the highest OH concentration of 69 ppm. At the fuel–air ratio of 0.25, the highest OH concentration is 182 ppm at the crankshaft angle of  $7.83^{\circ}\text{CA}$ . Equivalent combustion with EGR ratio of 68.1% has the highest OH concentration of 66 ppm at a crankshaft angle of  $5.97^{\circ}\text{CA}$ . Under the same load, the peak OH concentration of equivalent combustion is lower than that of lean combustion, but the crankshaft angle corresponding to the peak OH concentration decreases.

During the rapid combustion period, OH concentration increases rapidly with the increase in crankshaft angle. With the increase in the fuel–air ratio, the peak concentration of OH is higher, and the rise rate of OH concentration is faster, indicating that with the increase in the fuel to air ratio, the combustion in HICE is more rapid. During the expansion period, the concentration of OH decreases rapidly, because as an intermediate product of hydrogen–oxygen reaction, the temperature in the expansion period gradually decreases, and the reverse reaction gradually increases, resulting in the disappearance of OH with the end of the combustion in the cylinder.

During excessive hydrogen combustion, the concentration of OH decreases significantly compared to that of equivalent combustion, but the crankshaft angle with the peak OH concentration is earlier than that of equivalent combustion, and with the increase in excess hydrogen, the peak of OH concentration decreases and the crankshaft angle with

the peak of OH concentration decreases gradually. The in-cylinder concentration of H elements in excessive hydrogen combustion is high, which causes a large number of H and OH elements reactions and generates water quickly, reducing the concentration of OH.

According to the variation of peak OH concentration corresponding to crankshaft angle, it can be seen that under low load, equivalent combustion and excessive hydrogen combustion are more intense than lean combustion, and the intensity of combustion increases with the increase in excess hydrogen.

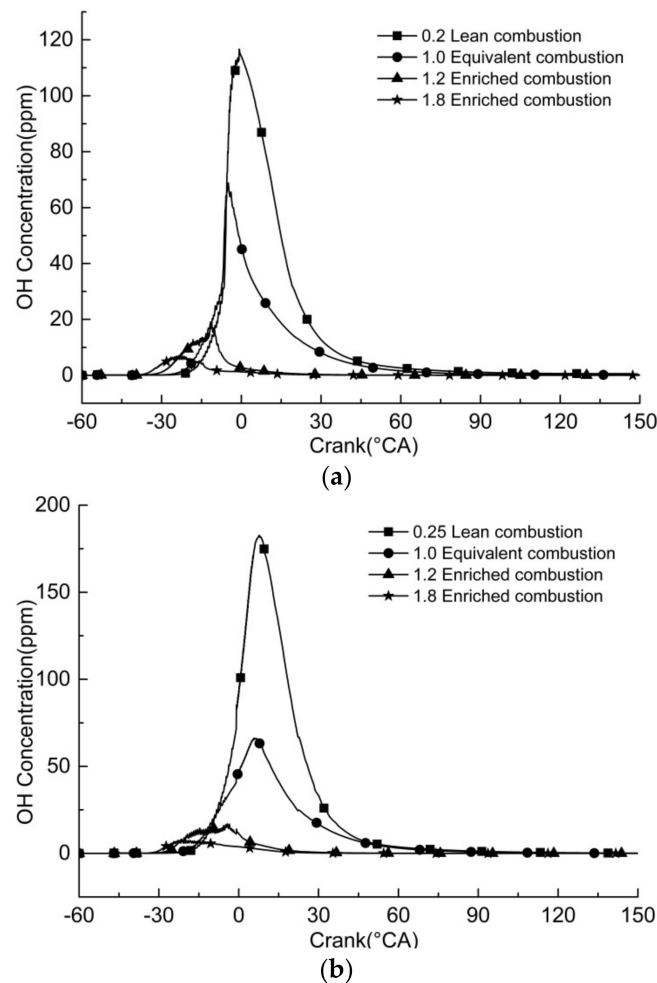


**Figure 4.** Variation of OH concentration in the cylinder change with the crankshaft angle in different combustion modes under low load. (a) Loading rate of 20%; (b) loading rate of 25%.

### 3.1.2. Variation of In-Cylinder Pressure

It can be seen in Figure 5 that the variation of in-cylinder pressure changes with crankshaft angle in different combustion modes under low load. It shows that at a loading rate of 20%, the maximum burst pressure in the cylinder is 3.59 MPa with the crankshaft angle 0.62 °CA; equivalent combustion occurs at the crankshaft angle of 0.56 °CA, and the maximum burst pressure in the cylinder is 3.60 MPa. When the fuel–air ratio is 1.8, the maximum burst pressure in the cylinder is 3.73 MPa at the crankshaft angle of  $-1.14$  °CA. While at the loading rate of 25%, the maximum explosion pressure is 3.64 MPa in the cylinder in lean combustion at a crankshaft angle of 7.17 °CA. Equivalent combustion occurs when the crankshaft angle is 7.07 °CA and the maximum burst pressure in the cylinder is 3.67 MPa. When the fuel–air ratio is 1.8, the maximum burst pressure in the cylinder is 4.27 MPa at the crankshaft angle of  $-0.75$  °CA. Under low load, the maximum burst pressure in equivalent combustion is slightly higher than that in lean combustion, and the crankshaft angle of the maximum burst pressure is smaller than that in lean combustion.

With the increase in excess hydrogen, the maximum burst pressure in the cylinder is higher than that in equivalent combustion, and the crankshaft angle of the maximum burst pressure decreases.

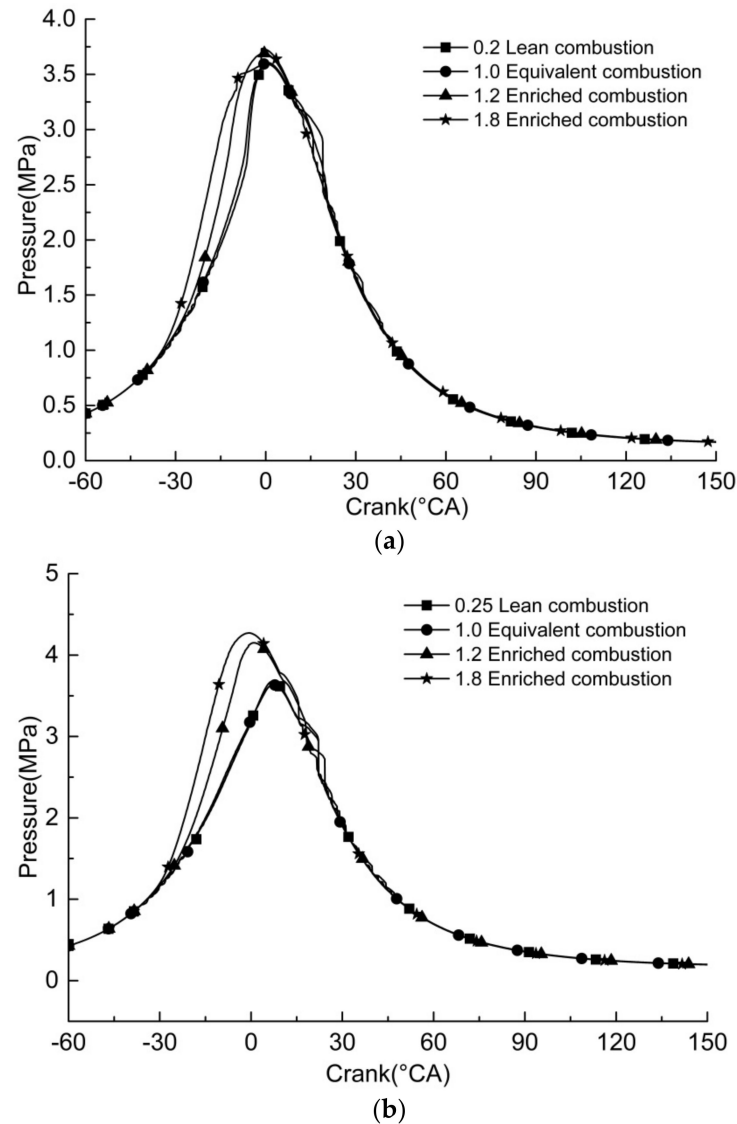


**Figure 5.** Variation of in-cylinder pressure change with the crankshaft angle in different combustion modes under low load. (a) Loading rate of 20%; (b) loading rate of 25%.

### 3.1.3. Variation of In-Cylinder Temperature

Figure 6 shows the variation of in-cylinder temperature changing with the crankshaft angle in different combustion modes under low load. It can be seen that when the loading rate is 20%, the in-cylinder temperature in lean combustion reaches the peak temperature of 1628 K at a crankshaft angle of 1.73 °CA, the peak value of which, in equivalent combustion, is 1635 K at a crankshaft angle of 1.47 °CA. The in-cylinder temperature in excessive hydrogen combustion at the fuel–air ratio of 1.2 reaches the peak temperature of 1680 K at a crankshaft angle of −2.76 °CA. The temperature in excessive hydrogen combustion at the fuel–air ratio of 1.8 reaches the peak temperature of 1707 K at a crankshaft angle of −5.22 °CA. While the loading rate is 25%, the peak temperature in lean combustion is 1686 K at a crankshaft angle of 11.26 °CA; the in-cylinder temperature in equivalent combustion reaches 1699 K at a crankshaft angle of 10.51 °CA. The temperature in excessive hydrogen combustion with the fuel–air ratio of 1.2 reaches the peak temperature of 1811 K

at the crankshaft angle of  $2.29^\circ\text{CA}$ . The temperature in excessive hydrogen combustion with the fuel–air ratio of 1.8 reaches the peak temperature of 1870 K at a crankshaft angle of  $-3.38^\circ\text{CA}$ .

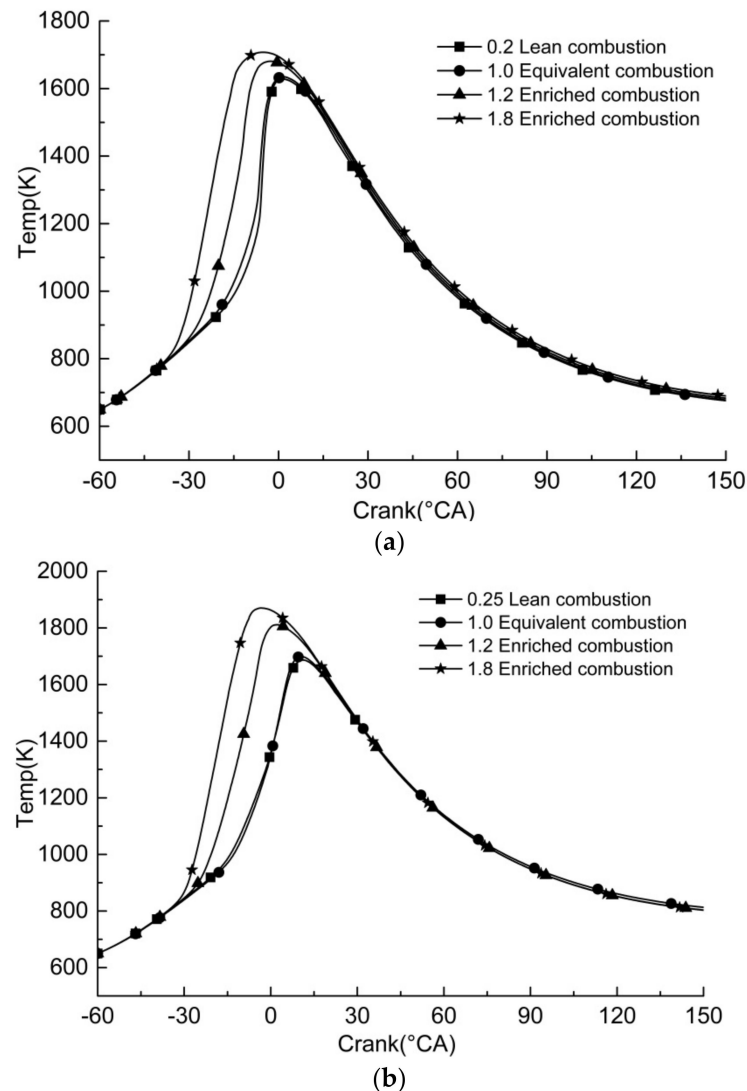


**Figure 6.** Variation of in-cylinder temperature change with the crankshaft angle in different combustion modes under low load. (a) Loading rate of 20%; (b) loading rate of 25%.

Under low load, the peak temperature in the cylinder increases with the increase in the fuel–air ratio, and the peak temperature of equivalent combustion is slightly higher than that of lean combustion; the corresponding crankshaft angle decreases. With the increase in excess hydrogen, the temperature peak increases and the corresponding crankshaft angle decreases. The results show that the intensity of combustion in HICE increases with the increase in the fuel–air ratio. The lower the mixture concentration is, the earlier the ignition time of MBT is; and the lower the mixture concentration is, the slower the combustion process is. The temperature also rises slowly, and the time at which the temperature reaches the peak is earlier. It is also shown that under low load, equivalent combustion appreciably improves the combustion condition in the cylinder. Concentrated combustion can improve the in-cylinder combustion condition under low load, and the intensity of combustion in the cylinder increases with the increase in excess hydrogen.

### 3.1.4. Variations of Indicated Power and Indicated Thermal Efficiency

Figure 7 shows the variations of indicated power and indicated thermal efficiency with dilution rate in different combustion modes under low load. At the loading rate of 20% the indicated power and indicated thermal efficiency in lean combustion are 11.36 kW and 44.13%, respectively, and the indicated power and indicated thermal efficiency in equivalent combustion are 11.39 kW and 44.20%, respectively. Meanwhile, at the loading rate of 25%, the indicated power and indicated thermal efficiency in lean combustion are 16.60 kW and 25.58%, respectively, and the indicated power and indicated thermal efficiency in equivalent combustion are 16.66 kW and 25.68%, respectively. The indicated power and indicated thermal efficiency in equivalent combustion are relatively slightly increased compared to those in lean combustion; the indicated power and indicated thermal efficiency of excessive hydrogen combustion are higher than those of equivalent combustion, and will increase gradually with the increase in excess hydrogen.

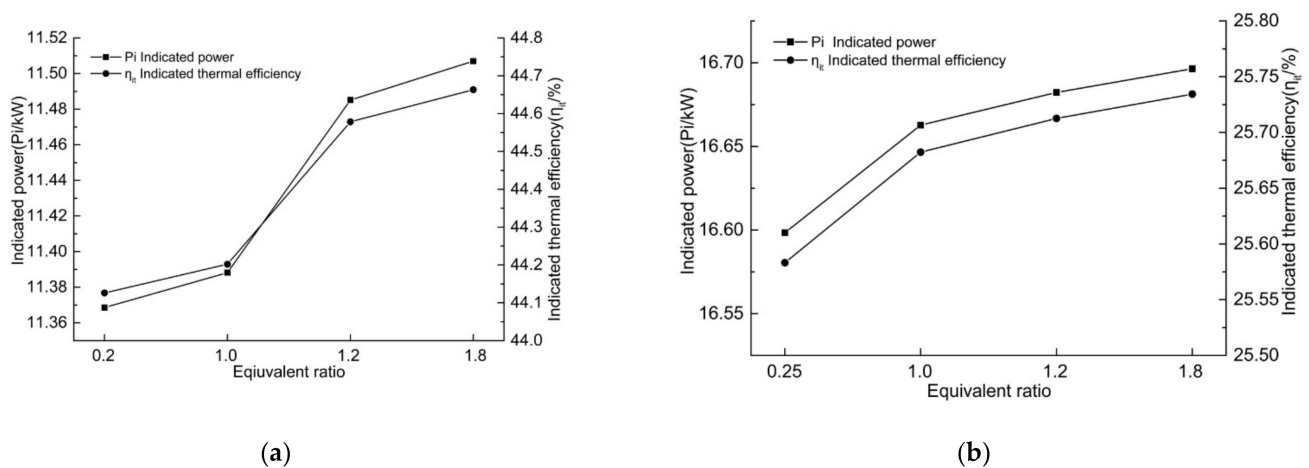


**Figure 7.** Variations of indicated power and indicated thermal efficiency in different combustion modes at low load. (a) Loading rate of 20%; (b) loading rate of 25%.

Under low load, the concentration of the mixture at the fuel–air ratio of 0.2 and 0.25 is too low, and the mixture spreads in the form of pellets in the combustion process without forming a continuous flame. The combustion temperature and pressure are low, and the combustion in the cylinder is slow, and the flame surface is discontinuous, and the partial transmission is slow in the form of fireballs [56]. Using equivalent combustion mode and excessive hydrogen combustion mode can promote the combustion in HICE under low load, increase the temperature and pressure in the cylinder, and then increase the indicating thermal efficiency of HICE.

### 3.2. Emission Characteristics and Mechanism

Under low load, the temperature and pressure in the cylinder of HICE are low, and the  $\text{NO}_x$  generation decreases. With the increase in fuel–air ratio, the  $\text{NO}_x$  emission of HICE will also increase. When the fuel–air ratio is too large, the  $\text{NO}_x$  emission of HICE is even higher than that of traditional internal combustion engine.  $\text{NO}$  element is the main  $\text{NO}_x$  emission ingredients of HICE, in addition also contains a small amount of  $\text{NO}_2$  and  $\text{N}_2\text{O}$  [57], the emission characteristics of HICE under low load are studied in this section.

#### 3.2.1. Distribution of NO Concentration during Rapid Combustion

Figure 8 shows the variation of in-cylinder  $\text{NO}$  concentration in different combustion modes under low load (Equations (1)–(10)). It can be seen that during the period of rapid combustion, the concentration of  $\text{NO}$  in the cylinder increases rapidly with the increase in the crankshaft angle and reaches a peak value. During the expansion period, as the crankshaft angle continues to increase, due to the decrease in the temperature in the cylinder,

part of the primitive reaction of generating NO appears to be the reverse reaction, and the concentration of NO decreases appreciably, but this has little influence on the generation of NO. When the temperature in the cylinder decreases to a certain value, the reverse reaction to generate NO does not continue, and the concentration of NO tends to be stable.

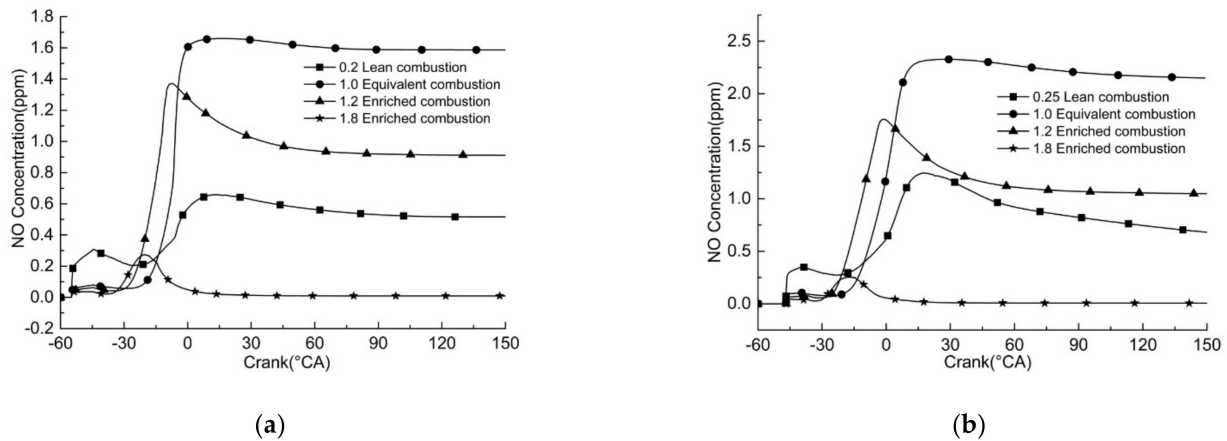


**Figure 8.** Variation of NO concentration in cylinder with crankshaft angle in different combustion modes under low load. (a) Loading rate of 20%; (b) loading rate of 25%.

Under low load, NO emission concentration in equivalent combustion increases to 2.15 ppm compared with lean combustion. With the increase in excess hydrogen, the concentration of NO in excessive hydrogen combustion decreases continuously, and the final NO emission concentration is less than 0.1 ppm. Under low load, the equivalent combustion is more intense than the lean combustion, and has a faster heat release rate and higher in-cylinder temperature, which promotes the formation of NO. The hydrogen content in the mixture of equivalent combustion and lean combustion is very low. Although hydrogen has higher activity than nitrogen, the reaction between nitrogen and oxygen increases in the reaction process due to the low hydrogen content, which promotes the generation of NO. The final concentration of NO is still at a very low level and has little influence on the emission of the internal combustion engine. In excessive hydrogen combustion, the amount of hydrogen in the mixture increases, and the more active hydrogen inhibits the formation of NO.

### 3.2.2. Formation of NO<sub>2</sub> and N<sub>2</sub>O

Besides NO, there are also small amounts of NO<sub>2</sub> and N<sub>2</sub>O in the emissions of HICE. Figures 9 and 10 are, respectively the variations of NO<sub>2</sub> concentration and N<sub>2</sub>O concentration in cylinder with the crankshaft angle in different combustion modes under low load.

It can be seen from Figure 9, that under the same load, NO<sub>2</sub> concentration slowly increases with the increase in the crankshaft angle; the peak concentration of NO<sub>2</sub> is 0.63 ppm at a fuel–air ratio of 0.25. The concentrations of NO<sub>2</sub> in all three combustion modes are no less than 0.2 ppm, which is a very low level.

As seen in Figure 10, during the rapid combustion period under the same load, the concentration of N<sub>2</sub>O increased sharply and reached the peak value, and continued to drop rapidly with the increase in the crankshaft angle. In three combustion modes under low load, although N<sub>2</sub>O fluctuates at a small crankshaft angle, the concentration of N<sub>2</sub>O generated during combustion is less than 0.6 ppm. According to the emission laws of NO, NO<sub>2</sub> and N<sub>2</sub>O, the emission of HICE is at a very low level at the fuel–air ratio of 0.2–0.25 under low load, and its emission characteristics have little influence.

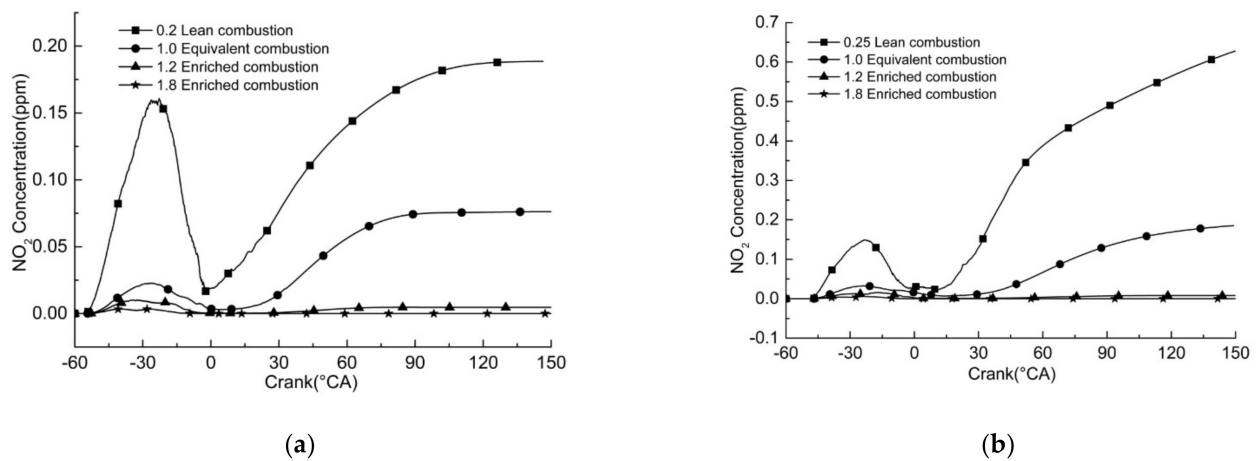


**Figure 9.** Variation of NO<sub>2</sub> concentration in the cylinder with crankshaft angle in different combustion modes under low load. (a) Loading rate of 20%; (b) loading rate of 25%.

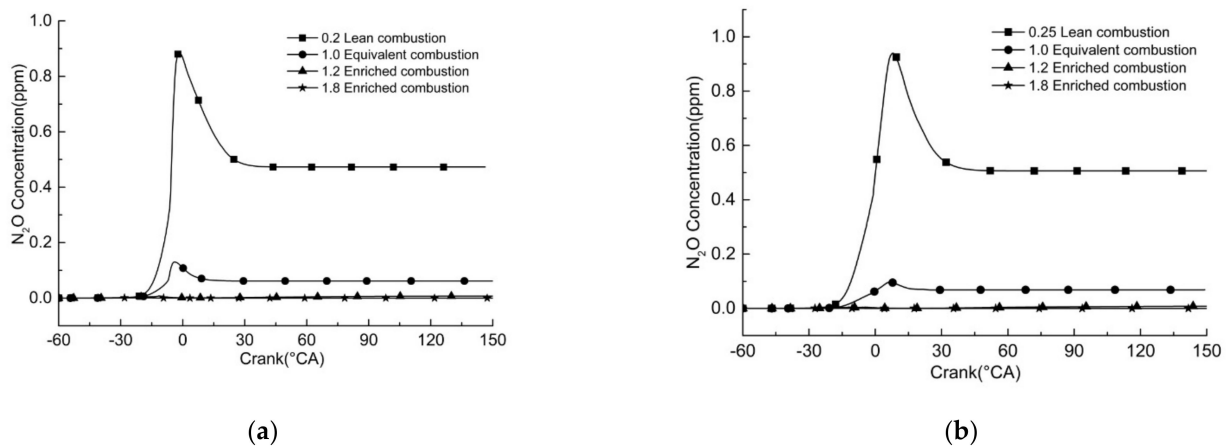


**Figure 10.** Variation of N<sub>2</sub>O concentration in the cylinder with crankshaft angle in different combustion modes under low load. (a) Loading rate of 20%; (b) loading rate of 25%.

#### 4. Conclusions

(1) Under low load, the OH concentrations in the cylinder of equivalent combustion and excessive hydrogen combustion are lower than in lean combustion. With the increase in excess hydrogen, the OH concentration decreases accordingly; however, the crankshaft angle corresponding to the peak OH concentration decreases. It can be indicated that both equivalent combustion and excessive hydrogen combustion burn more intensely than lean combustion, and their combustion intensities increase with the increase in excess hydrogen under low load.

(2) With the increase in excess hydrogen, the adoption of equivalent combustion and excessive hydrogen combustion can promote the intensity of combustion of HICE under low load. The peak values of temperature and pressure in the cylinder increase gradually, and the indicated power and indicated thermal efficiency are also higher. The peak values of temperature and pressure in equivalent combustion are slightly higher than that of lean combustion; nevertheless, the peak values of temperature and pressure in excessive hydrogen combustion rise sharply, and the rising rate reaches up to 10% and 16%.

(3) NO is the main component of NO<sub>x</sub> emission of HICE. Under low load in three combustion modes, the peak NO concentration is 2.15 ppm at the fuel–air ratio of 0.25, and the emissions of NO<sub>2</sub> and N<sub>2</sub>O are always small. The total generation of NO<sub>x</sub> is at a very low level, which has little effect on the emission performance.

In summary, equivalent combustion and excessive hydrogen combustion with medium-cooled EGR dilution can improve the intensity of in-cylinder combustion of HICE, reduce the possibility of in-cylinder fire, and improve the indicated thermal efficiency under low load. However, larger excessive hydrogen combustion could weaken the improvement of the performance, and a large amount of hydrogen in the mixture gas does not participate in combustion but is discharged with the exhaust gas, which greatly reduces the utilization of hydrogen and economy of HICE. Therefore, the performance of HICE could be comprehensively improved by the adoption of excessive hydrogen combustion with the fuel–air ratio below 1.2 under low load.

**Author Contributions:** Conceptualization, W.W. and H.Z.; methodology, J.D. and H.Z.; validation, X.H., H.Z. and J.D.; investigation, W.W. and H.Z.; writing—original draft preparation, W.W. and H.Z.; writing—review and editing, W.W. and H.Z.; visualization, G.Q.; funding acquisition, X.H. and H.Z. All authors have read and agreed to the published version of the manuscript.

**Funding:** This research was funded the by National Natural Science Foundation of China, grant number 51976012, 51706058; Science and Technology Project of Hebei Education Department, grant number ZD 2019101.

**Institutional Review Board Statement:** Not applicable.

**Informed Consent Statement:** Not applicable.

**Data Availability Statement:** Not applicable.

**Conflicts of Interest:** The authors declare no conflict of interest.

## References

- British Petroleum Company. BP World Energy Yearbook. Available online: [https://www.bp.com/zh\\_cn/china/reports-and-publications/\\_bp2017.html](https://www.bp.com/zh_cn/china/reports-and-publications/_bp2017.html) (accessed on 5 May 2017).
- Wang, J. Urban automobile exhaust emission and environmental pollution and its prevention and control countermeasures. *Sci. Technol. Inf.* **2013**, *1*, 445–446.
- Xing, L.; Su, X. Spatial and temporal distribution characteristics of air quality index in Central Plains Urban agglomeration. *J. North China Univ. Water Resour. Electr. Power (Soc. Sci. Ed.)* **2017**, *33*, 38–44.
- Beatty, T.; Shimshack, J.P. Air pollution and children’s respiratory health: A cohort analysis. *J. Environ. Econ. Manag.* **2014**, *67*, 39–57. [CrossRef]
- Jacquemin, B.; Kauffmann, F.; Pin, I.; Le Moual, N.; Bousquet, J.; Gormand, F.; Just, J.; Nadif, R.; Pison, C.; Vervloet, D.; et al. Air pollution and asthma control in the epidemiological study on the genetics and environment of asthma. *J. Epidemiol. Community Health* **2012**, *66*, 796. [CrossRef]
- Meng, X.; Wang, C.; Cao, D.; Wong, C.-M.; Kan, H. Short-term effect of ambient air pollution on COPD mortality in four Chinese cities. *Atmos. Environ.* **2013**, *77*, 149–154. [CrossRef]
- Gauderman, W.J.; Vora, H.; McConnell, R.; Berhane, K.; Gilliland, F.; Thomas, D.; Lurmann, F.; Avol, E.; Kunzli, N.; Jerrett, M.; et al. Effect of exposure to traffic on lung development from 10 to 18 years of age: A cohort study. *Lancet* **2007**, *369*, 571–577. [CrossRef]
- Kheirbek, I.; Wheeler, K.; Walters, S.; Kass, D.; Matte, T. PM<sub>2.5</sub> and ozone health impacts and disparities in New York City: Sensitivity to spatial and temporal resolution. *Air Qual. Atmos. Health* **2013**, *6*, 473–486. [CrossRef]
- Liu, X. On the prospect of non-petroleum fuel vehicle engine. *Automob. Technol.* **2002**, *3*, 13–14.
- Mao, Z. *Hydrogen-Green Energy of 21st Century*; Chemical Industry Press: Beijing, China, 2005; pp. 24–29.
- Zhang, Q. *Experimental Investigation on the Combustion and Emission Characteristics of Alcohol-Fueled Engine with Hydrogen Addition*; Beijing University of Technology: Beijing, China, 2017.
- Junjun, Z.; Xinqi, Q.; Zhen, W.; Bin, G.; Zhen, H. Experimental investigation of low temperature combustion (ltc) in an engine fueled with dimethyl ether (DME). *Energy Fuels* **2009**, *23*, 170–174. [CrossRef]
- Wang, Y.; Guo, Z.; He, L.; Li, W.; Zhou, L. Study on PCCI-DI combustion in dimethyl ether engine. *Trans. Csice* **2008**, *4*, 170–174.
- Li, B. Research progress of methanol and dimethyl ether as alternative fuels. *Shanghai Auto* **2004**, *5*, 36–39.
- Wu, J.; Wu, J.; Liu, H. Research status and prospect of methanol as alternative fuel for diesel engines. *Energy Conserv. Technol.* **2021**, *39*, 9–14.
- Gao, Y. *The Research of the Effects of Alcohol Fuel on the Single-Cylinder Two-Stroke Gasoline Engine*; Beijing Forestry University: Beijing China, 2010.
- Ke, W. Vigorously develop alcohol fuels to replace traditional energy. *Chin. J. Bioeng.* **2007**, *3*, 501.
- Liu, Z. *Feasibility Analysis of Based Alternative Fuel Vehicles*; Jilin University: Jilin, China, 2004.

19. Wang, J. *Investigation into In-Cylinder Gas Movement and Combustion of Dme Engine*; Shanghai Jiao Tong University: Shanghai, China, 2016.
20. Han, Z. Rationality analysis of dimethyl ether as alternative fuel. *Shandong Chem. Ind.* **2014**, *43*, 115–117.
21. Zhang, W. *Research on Characteristics of Diaphragm Pump for the Fuel Injection System of Dimethyl ether Engine*; Wuhan University of Science and Technology: Wuhan, China, 2011.
22. Huang, J. Dimethyl ether replaces automotive fuel to speed up the process. *China Environ. News* **2006**, *7*, 18.
23. Xiao, Y. Energy conservation and emission reduction drive the promising natural gas vehicle market. *New Mater. Ind.* **2010**, *7*, 63–67.
24. Grzesik, Z.; Smola, G.; Adamaszek, K. High temperature corrosion of valve steels in combustion gases of petrol containing ethanol addition. *Corros. Sci.* **2013**, *77*, 369–374. [[CrossRef](#)]
25. Thiruvengadam, A.; Besch, M.; Padmanaban, V.; Pradhan, S.; Demirgok, B. Natural gas vehicles in heavy-duty transportation—a review. *Energy Policy* **2018**, *122*, 253–259. [[CrossRef](#)]
26. Chong, Z.R.; Yang, S.H.B.; Babu, P.; Linga, P.; Li, X.S. Review of natural gas hydrates as an energy resource: Prospects and challenges. *Appl. Energy* **2016**, *162*, 1633–1652. [[CrossRef](#)]
27. Du, G. *Study on the Expansion of High Efficiency and Stable Operation Range of Compression Ignition Natural Gas Engine*; Jilin University: Jilin, China, 2021.
28. Lin, L.; Xu, M. Effect of initial temperature on combustion characteristics of biomass diesel oil. *Fire Sci. Technol.* **2019**, *38*, 462–464.
29. Wang, C.; Cui, F.; Song, Y. Research status and development prospect of biodiesel. *China Oils Fats* **2014**, *39*, 44–48.
30. Bai, X. *Study on Combustion and Emissions Characteristics of a Hydrogen Fueled Internal Combustion Engine under Cold Start Conditions*; Beijing University of Technology: Beijing, China, 2019.
31. Zhang, Y.; Luo, Q.; Liu, F. Research Status and Prospect of Hydrogen Fuel internal Combustion Engine. *Small Internal Combust. Engine Motorcycle* **2007**, *36*, 70–73.
32. Zhao, P.; Zhang, H. analysis of application prospect for hydrogen combustion engines. *China Resour. Compr. Util.* **2020**, *38*, 72–74.
33. Yilancı, A.; Dincer, I.; Ozturk, H.K. A review on solar-hydrogen/fuel cell hybrid energy systems for stationary applications. *Prog. Energy Combust. Sci.* **2009**, *35*, 231–244. [[CrossRef](#)]
34. Yu, C.; Zhang, X.; Zhang, K.; Liu, Y.; Shen, Y. Application and development of small hydrogen fuel cell. *Chin. Battery Ind.* **2021**, *25*, 317–320.
35. Zhu, Y.; Huang, X.; Chen, H.; Ni, P.; Zhang, X. Development status and prospect of hydrogen internal combustion engine. *Mod. Chem. Res.* **2021**, *24*, 5–7.
36. Xu, H. Application status and development trend of hydrogen fuel cell technology. *Sci. Technol. Innov.* **2019**, *2*, 160–161.
37. Wang, Y. *Numerical Simulation of Fatigue Crack Growth of Proton Exchange Membrane for Hydrogen Fuel Cells*; Tianjin University: Tianjin, China, 2020.
38. Cheng, Y. Application status and development trend of hydrogen fuel cell technology. *Green Pet. Petrochem.* **2018**, *3*, 5–13.
39. Sun, B.; Bao, L.; Luo, Q. Development and Trends of Direct Injection Hydrogen Internal Combustion Engine Technology. *J. Automot. Saf. Energy* **2021**, *12*, 265–278.
40. Yao, F.; Jia, Y.; Mao, Z.Q. The cost analysis of hydrogen life cycle in China. *Int. J. Hydrogen Energy* **2010**, *35*, 2727–2731. [[CrossRef](#)]
41. Wang, L.; Yang, Z.; Si, A.; Ge, L. Development and prospect of hydrogen fuel internal combustion engine. *Small Intern. Combust. Engines Motorcycl.* **2009**, *35*, 230–244.
42. Ma, F.; Liu, H.; Li, Y.; Wang, Y.; Zhao, S. Internal combustion characteristics of hydrogen internal combustion engine. *Intern. Combust. Engine Eng.* **2008**, *1*, 29–33.
43. Sun, B.; Zhang, D.; Liu, F. Cycle variation characteristics of hydrogen internal combustion engine. *Combust. Sci. Technol.* **2013**, *19*, 311–316.
44. Sun, B.; Zhang, D.; Liu, F. Evaluation method for cycle variation characteristics of hydrogen internal combustion engine. *Trans. CSICE* **2013**, *31*, 133–138.
45. Ji, C.; Yan, H.; Wang, S.; Zhang, Q.; Zhang, M.; Zhou, X. Simulation study on thin combustion performance of gasoline mixed hydrogen Internal combustion Engine. *J. Beijing Univ. Technol.* **2012**, *38*, 417–422.
46. Sun, D.; Liu, F.; Sun, B.; Zhou, L. Experimental study on the effect of hot EGR on performance and emission of hydrogen combustion engine. *Trans. CSICE* **2009**, *27*, 134–139.
47. Ren, T.; Guo, H.; Chu, C. Effect of different EGR on combustion characteristics of hydrogen internal combustion engine. *Automob. Appl. Technol.* **2014**, *2*, 29–32.
48. Liu, F. *CFD Study on Hydrogen Engine Mixture Formation and Combustion*; Cuvillier Press: Goettingen, Germany, 2004.
49. Duan, J. *Combustion and Emission Formation Mechanisms of Hydrogen Fueled Internal Combustion Engine under Dilution Condition*; Beijing Institute of Technology: Beijing, China, 2015.
50. Fan, Y. *Study on Combustion and Emission Characteristics of Hydrogen under Thermal EGR*; Beijing Institute of Technology: Beijing, China, 2016.
51. Hao, J.; Sun, B. Research on improving the compression ratio of hydrogen internal combustion engines by using exhaust gas recirculation and miller cycle. *Chin. Intern. Combust. Engine Eng.* **2021**, *42*, 52–59.

52. Sharma, P.K.; Sharma, D.; Soni, S.L.; Jhalani, A.; Singh, D.; Sharma, S. Characterization of the hydrogen fueled compression ignition engine under dual fuel mode: Experimental and numerical simulation. *Int. J. Hydrogen Energy* **2020**, *45*, 8067–8081. [[CrossRef](#)]
53. Sharma, P.K.; Sharma, D.; Soni, S.L.; Jhalani, A.; Singh, D.; Sharma, S. Energy, and emission analysis of a hydroxyl fueled compression ignition engine under dual fuel mode. *Fuel* **2020**, *265*, 116923. [[CrossRef](#)]
54. Sun, D.; Liu, F. Research on the performance and emission of a port fuel injection hydrogen internal combustion engine. In Proceedings of the International Conference on Computer Distributed Control and Intelligent Environmental Monitoring, Changsha, China, 19–20 February 2011; pp. 963–966.
55. Duan, J.; Yang, Z.; Sun, B.; Chen, W.; Wang, L. Study on the NO<sub>x</sub> emissions mechanism of an HICE under high load. *Int. J. Hydrog. Energy* **2017**, *42*, 22027–22035. [[CrossRef](#)]
56. Sun, B.; Zhao, J.; Zhao, L. Experimental study on NO<sub>x</sub> emission characteristics of hydrogen combustion engine. *Intern. Combust. Engine Eng.* **2011**, *32*, 53–56.
57. Conaire, M.Ó.; Curran, H.J.; Simmie, J.M.; Pitz, W.J.; Westbrook, C.K. A comprehensive modeling study of hydrogen oxidation. *Int. J. Chem. Kinet.* **2004**, *36*, 603–622. [[CrossRef](#)]